Supporting Information for "Barchan dunes on bidispersed granular beds"

C. A. Alvarez[1,2], F. D. Cúñez[1], E. M. Franklin[1]

[1]School of Mechanical Engineering, UNICAMP - University of Campinas,

Rua Mendeleyev, 200, Campinas, SP, Brazil

[2]Department of Atmospheric and Oceanic Sciences, University of California, Los Angeles,

Los Angeles, CA 90095-1565, USA

Contents of this file

1. Figures S1 to S11

2. Tables S1 and S2

Additional Supporting Information (Files uploaded separately)

1. Captions for Movies S1 to S4

Introduction

This supporting information presents the layout of the experimental device, microscopy images of the used grains, snapshots of barchans of different grain types, additional graphics of grain trajectories, and movies showing examples bidispersed barchan evolutions. For the latter, we present top view movies for different densities, different sizes, and different

December 6, 2020, 11:56am

densities and sizes, and a side view movie for different grain sizes. All movies have been sped up by 2x. We note that individual images and movies used in the manuscript are available on Mendeley Data (https://data.mendeley.com/datasets/z42c97sw4c).

The experiments described in the paper were conducted in a water channel of transparent material, for which the layout is shown in Figure S1. With the channel previously filled with water, controlled grains were poured inside, forming conical piles consisting of bidispersed grains that were afterward deformed into a barchan dune by imposing a water flow.

We used two cameras of complementary metal-oxide-semiconductor (CMOS) type. One, placed above the channel, acquired top view images of the bedform while the other, placed horizontally, acquired side-view images. The resolution of both cameras was of 1920 px × 1080 px at 60 Hz and they were mounted on a traveling system. The regions of interest (ROI) were set to 1920 px × 941 px and 1280 px × 241 px for the top and lateral cameras, respectively, and the frequency to 60 Hz. We used lenses of 18 - 140 mm and 18 - 105 mm focal distances mounted on the top and lateral cameras, respectively, and lamps of light-emitting diode (LED) were branched to a continuous-current source to provide the necessary light while avoiding beating. The conversion from px to a physical system of units was made based on images of a scale placed in the channel previously filled with water. The acquired images were afterward processed by numerical scripts written in the course of this work.

Movie S1.Case_e_2x.mp4 Top view movie of the evolution of a barchan consisting of bidispersed grains with different densities

Movie S2. Case_h_2x.mp4 Top view movie of the evolution of a barchan consisting of bidispersed grains with different sizes

Movie S3. Case_q_2x.mp4 Top view movie of the evolution of a barchan consisting of bidispersed grains with different densities and sizes

Movie S4. Case_h_sideview_2x.mp4 Side view movie of the evolution of a barchan consisting of bidispersed grains with different sizes
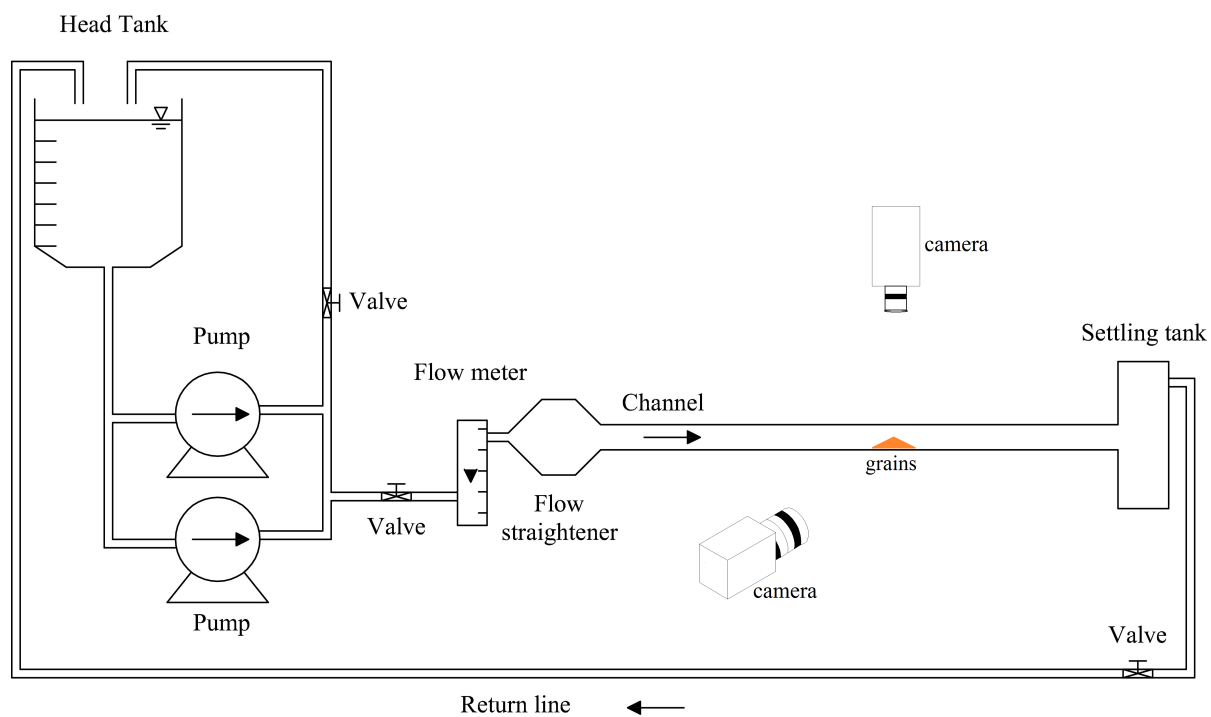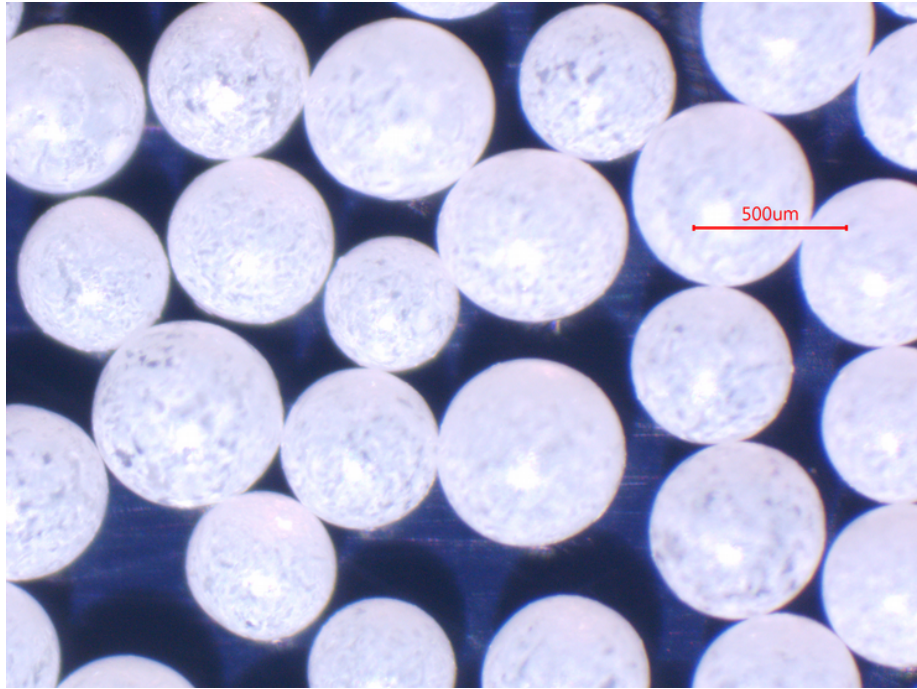
Figure S1. Layout of the experimental setup.

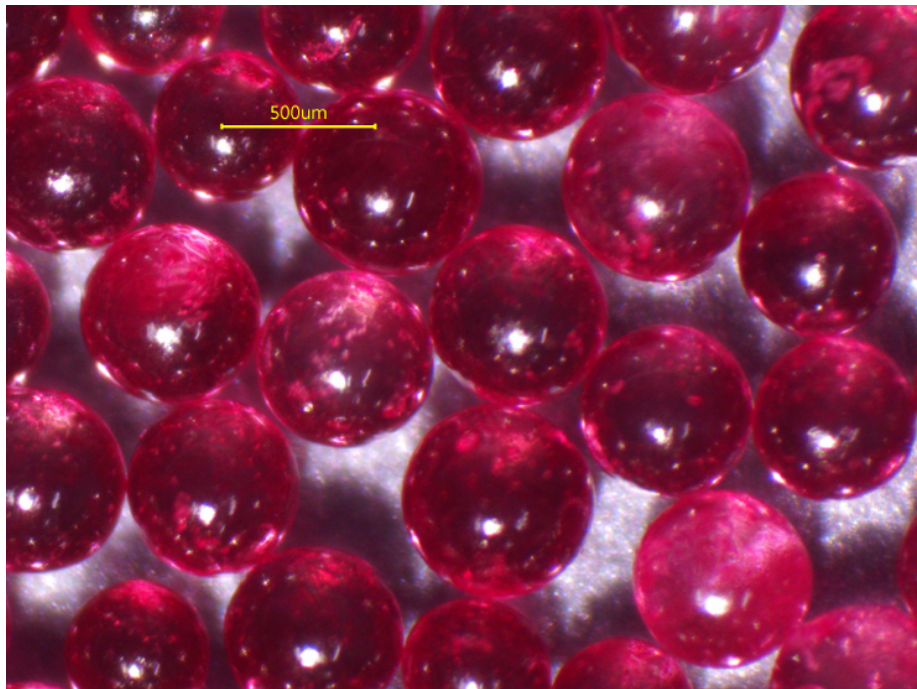**Figure S2.** Microscopy image for the 0.40 mm $\leq d \leq$ 0.60 mm round glass beads of white color.

Figure S3. Microscopy image for the 0.40 mm $\leq d \leq$ 0.60 mm round glass beads of red color.

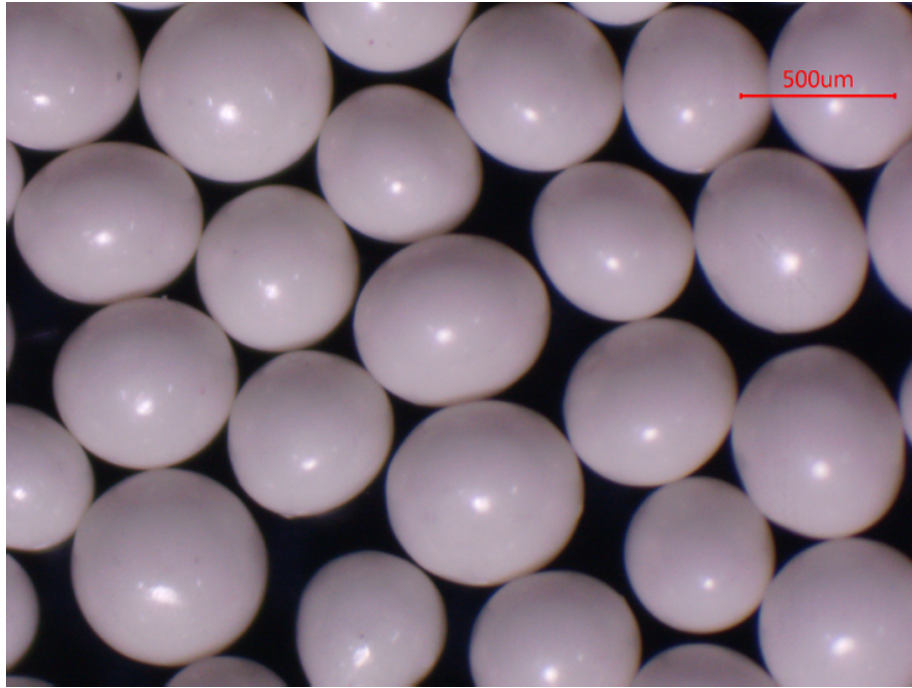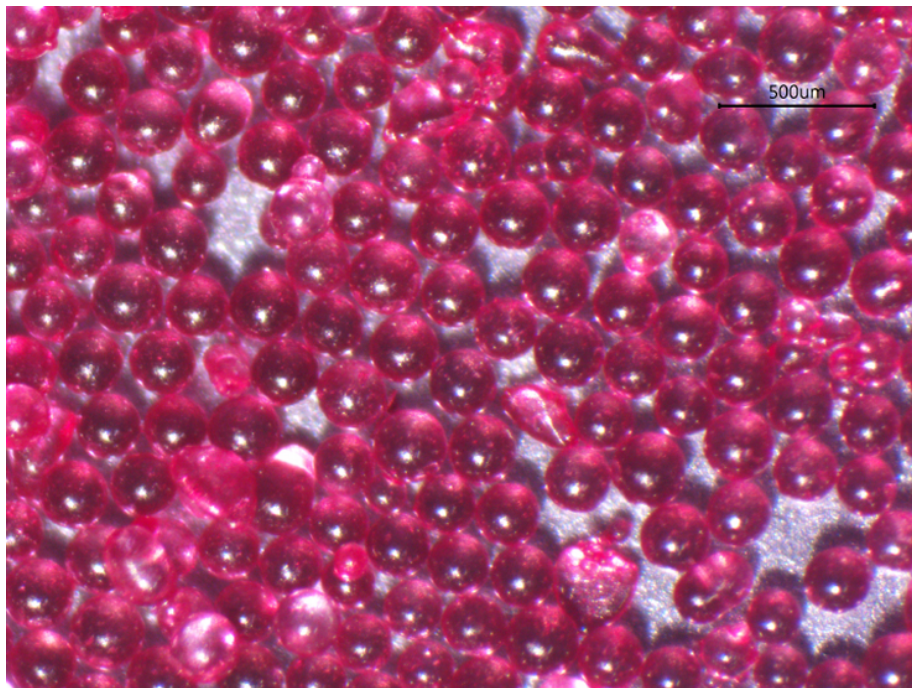**Figure S4.** Microscopy image for the 0.40 mm $\leq d \leq$ 0.60 mm round zirconia beads.

Figure S5. Microscopy image for the 0.15 mm $\leq d \leq$ 0.25 mm round glass beads of red color.
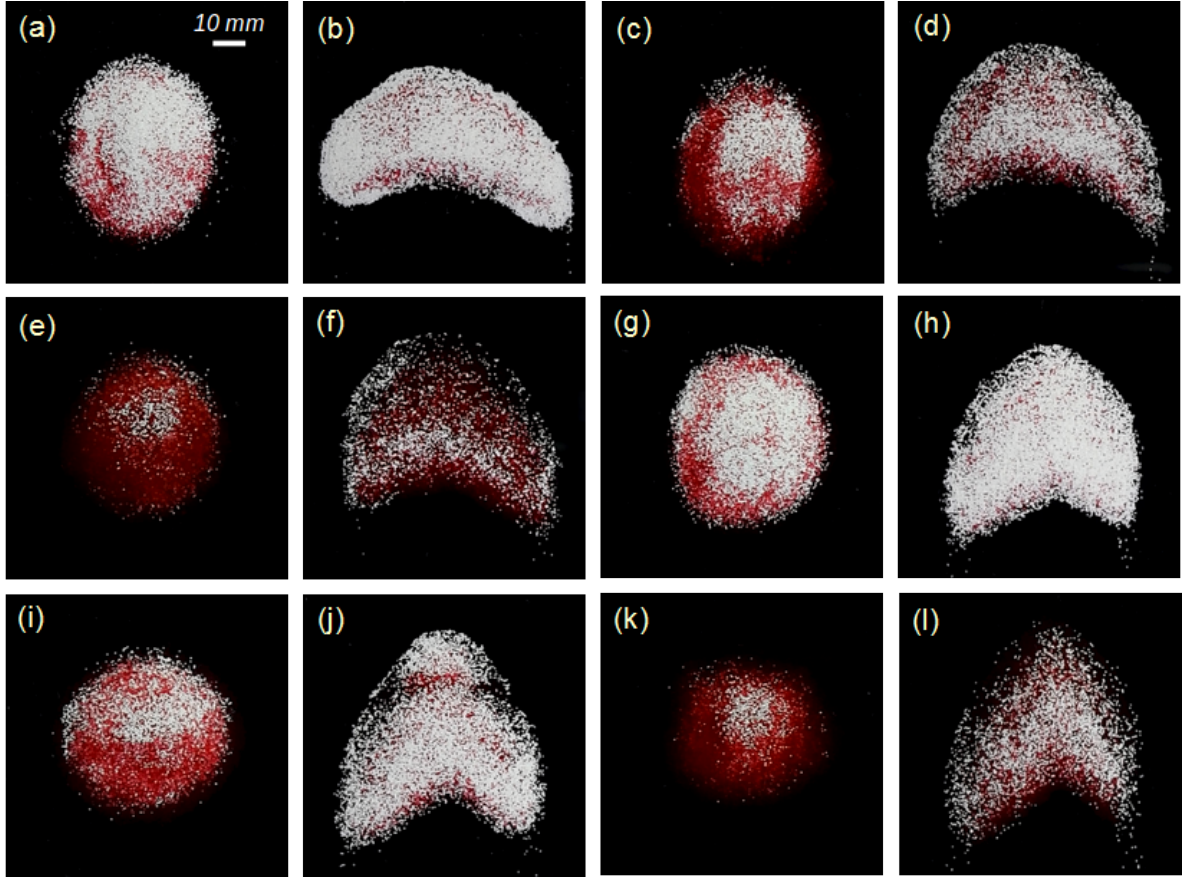
Figure S6. Top view of the initial pile and barchan dune for dunes of different densities and same diameter. Figures (a) and (b) to (k) and (l), by pairs, correspond to the initial pile and barchan, respectively, of cases a to f.
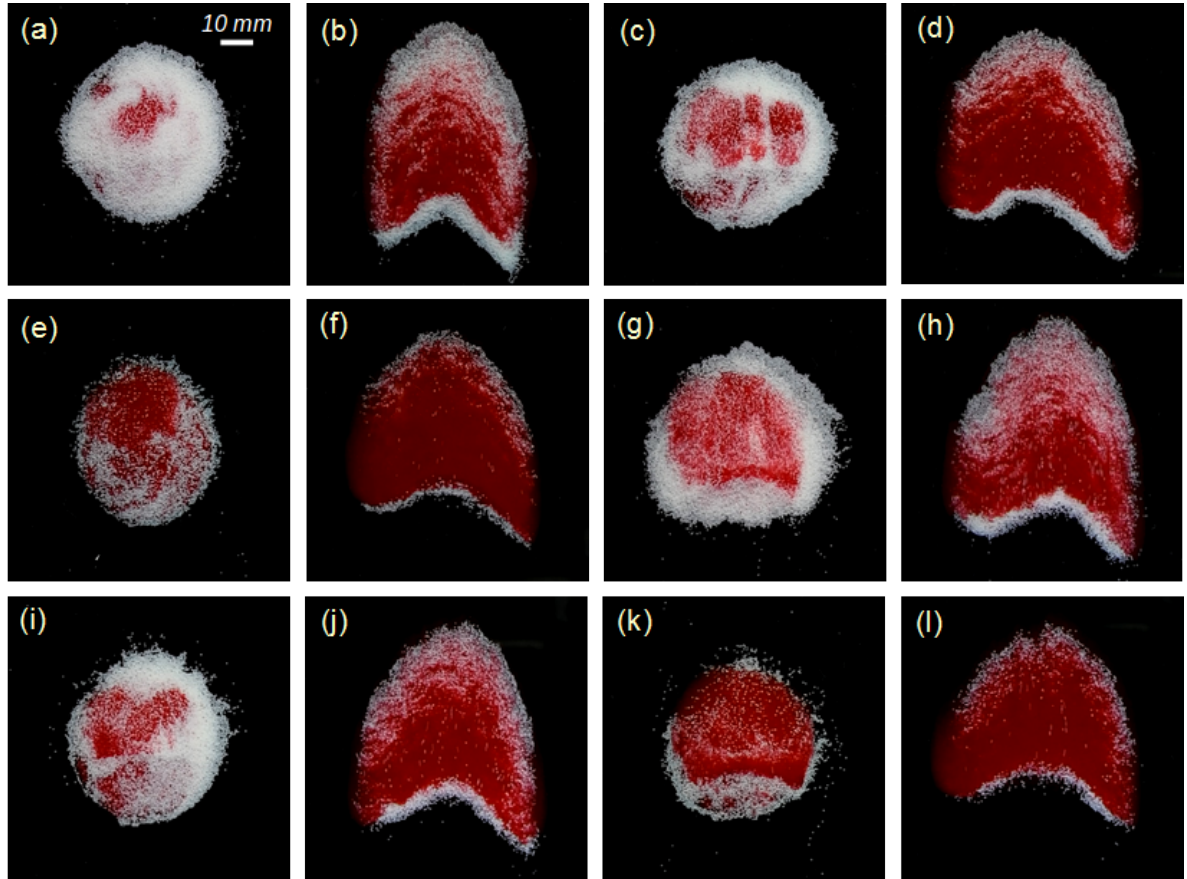
Figure S7. Top view of the initial pile and barchan dune for dunes of same density and different diameters. Figures (a) and (b) to (k) and (l), by pairs, correspond to the initial pile and barchan, respectively, of cases g to l.
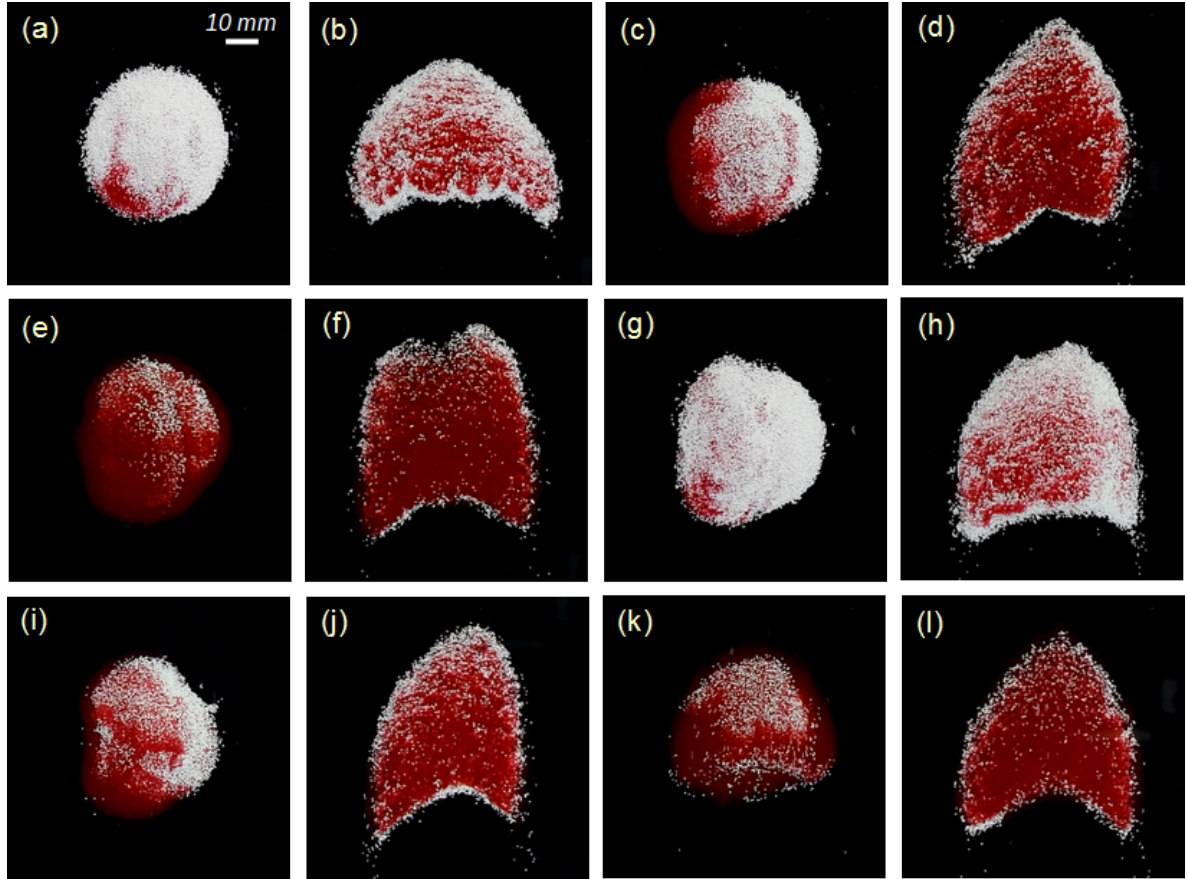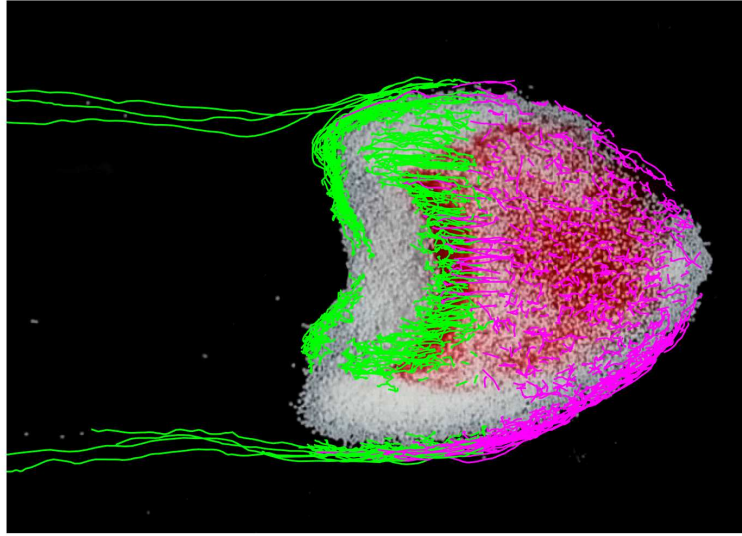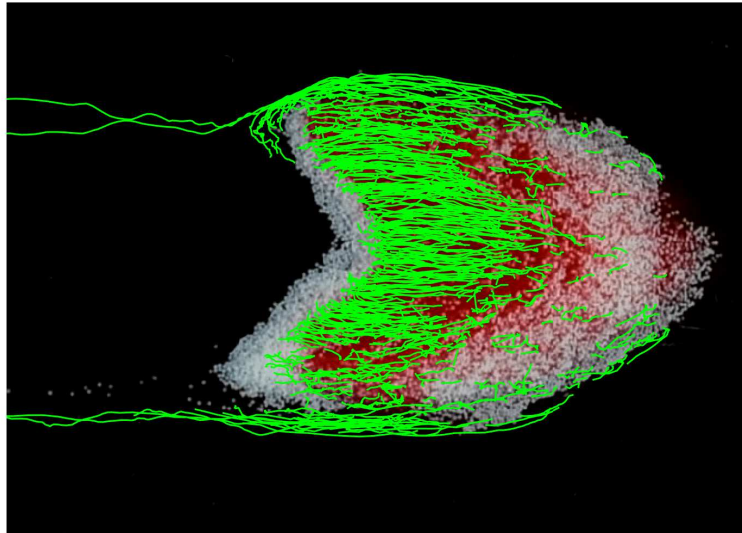
Figure S8. Top view of the initial pile and barchan dune for dunes of different densities and diameters. Figures (a) and (b) to (k) and (l), by pairs, correspond to the initial pile and barchan, respectively, of cases m to r.
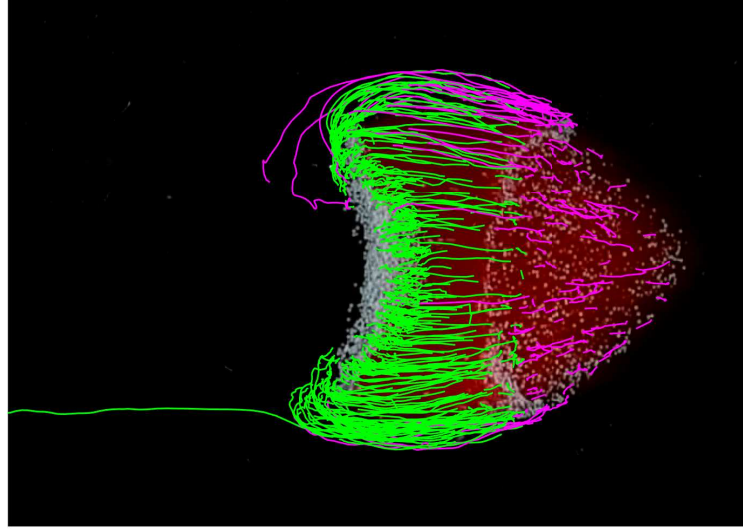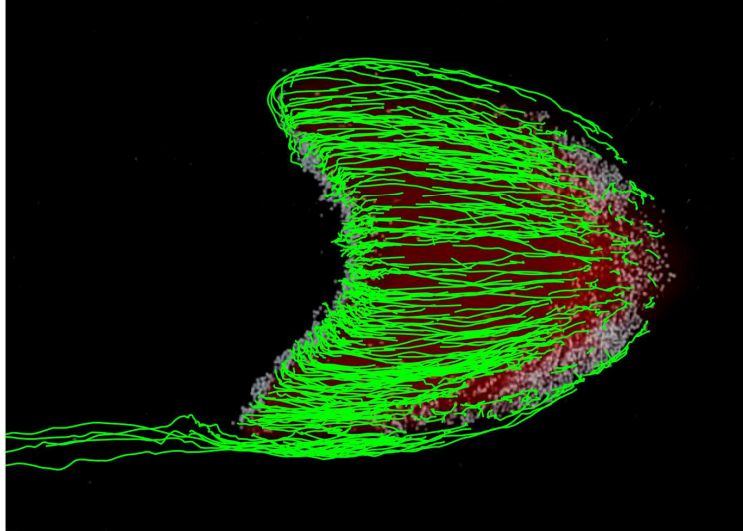
(a)

(b)

Figure S9. Trajectories of larger grains of case g, for two different intervals: Figure (a), from $t = 25$ to 65 s, when the stripe was still present, and Figure (b), from $t = 170$ to 210 s, when it had already vanished. In Figure (a), green lines correspond to grains that started moving in positions downstream the transverse stripe, while magenta lines correspond to those that started moving in position upstream the stripe. In the figure, flow is from right to left

(a)

(b)

Figure S10. Trajectories of larger grains of case i, for two different intervals: Figure (a), from $t = 40$ to 80 s, when the stripe was still present, and Figure (b), from $t = 150$ to 190 s, when it had already vanished. In Figure (a), green lines correspond to grains that started moving in positions downstream the transverse stripe, while magenta lines correspond to those that started moving in position upstream the stripe. In the figure, flow is from right to left
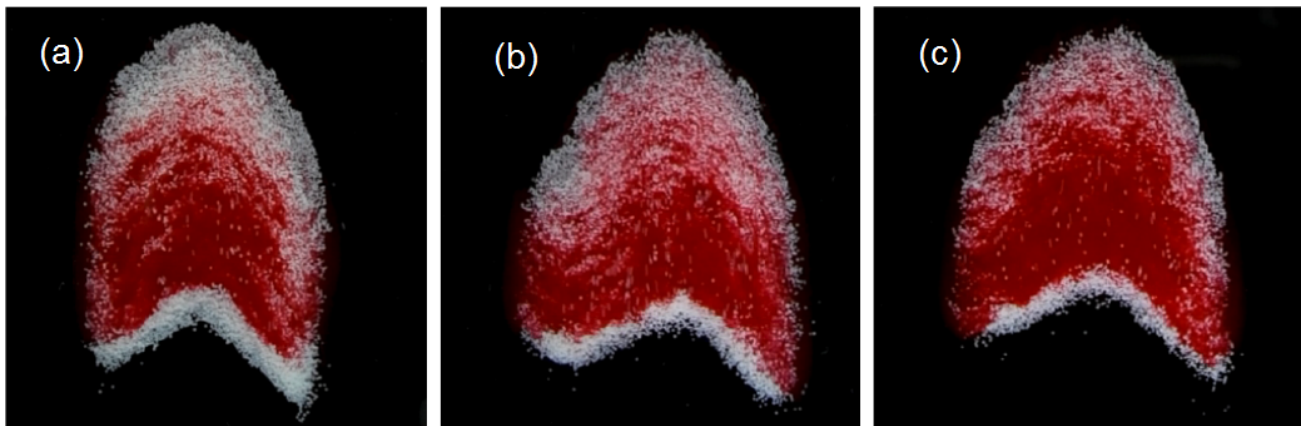
Figure S11. Examples of oblique stripes observed on some dunes. (a) Case g at $t = 240$ s. (b) Case j at $t = 120$ s. (c) Case k at $t = 130$ s.

Table S1. Values of Re$_*$ and θ for each species and flow conditions.

Species	Re	Re$_*$	θ
S_1	$1.47{\times}10^4$	8	0.02
S_1	$1.82{\times}10^4$	10	0.03
S_2	$1.47{\times}10^4$	8	0.04
S_2	$1.82{\times}10^4$	10	0.06
S_3	$1.47{\times}10^4$	3	0.10
S_3	$1.82{\times}10^4$	4	0.14

Table S2. Arithmetic mean of the wavelengths of oblique stripes, λ for cases g, h, j and k.

Case	λ	λ/d
$\cdots$	(mm)	$\cdots$
g	2.4	13
h	3.1	16
j	2.5	13
k	2.7	14